Effect of the bending modes on the radiated sound pressure from a submarine hull

Mauro Caresta, Nicole Kessissoglou
School of Mechanical and Manufacturing Engineering, The University of New South Wales, Sydney, NSW 2052, Australia

ABSTRACT

Rotation of the propeller through a non-uniform wake results in fluctuating forces transmitted through the propulsion system to the hull of a submerged vessel. The axial component of the fluctuating harmonic forces excites the axi-symmetric modes of the submarine while the component in the radial direction is shown to primarily excite the bending modes of the submarine. The hull is surrounded by water and is modelled as a cylindrical shell with internal bulkheads, ring stiffeners and truncated conical end caps. The structure-borne radiated sound pressure was calculated using the Helmholtz integral formulation. Structural and acoustics results from both the semi-analytical model and a fully coupled finite element/boundary element model are presented.

INTRODUCTION

Fluctuating forces due to rotation of the propeller excite the low frequency vibration modes of a submerged vessel, resulting in a high level of radiated noise. Understanding the low frequency vibro-acoustic responses of a submarine is of great interest in order to prevent detection problems of defence vessels.

The Helmholtz integral formulation is a powerful tool to calculate the sound pressure radiated from elastic structures. However, only a small number of simple structures such as spherical shells and infinitely periodic cylinders allow an analytical solution (Junger and Feit, 1986). Many researchers have investigated approximate methods to solve the acoustic radiation from elastic structures. Finite element methods were used in some early papers (Alfredson 1973; Arlett et al. 1968), but the boundary integral equation formulation has become more popular. A comprehensive review on the evolution of boundary element techniques is given by Chien et al. (1990). Variational principle has also been used to solve radiation problems (Wu 1989; Chen and Ginsberg 1993; Bjarnason et al. 1994; Choi et al. 1995). Chen and Stepanishen (1994) proposed a new method based on an *in vacuo* modal expansion to solve fluid loaded shells. Coupled finite element/boundary element methods have been presented by Jeans and Mathews (1990, 1993) to study the vibrations of structures in an infinite acoustic medium. A variety of techniques to examine the sound radiation from slender bodies of revolution and spheroidal shells have often been developed with application to submarine hulls (Chertock 1975; Stepanishen 1997; Hue-Wang and Stepanishen 1994; Pei-Tai and Ginsberg 1993; Achenbach et al. 1992; Choi et al. 1996; Pond 1966). Recently, Pan et al. (2008a, 2008b) studied an active control strategy to reduce the sound radiation from an axisymmetrically vibrating submarine vessel with conical and spherical end caps.

In this work, the pressure radiated from a submarine hull is presented. The hull is modelled as a finite cylindrical shell closed at each end by truncated conical end caps. The contribution from both the cylindrical hull and cones are taken into account in evaluating the radiated sound pressure. Imperfections from the propulsion system result in fluctuating forces in both the axial and radial directions. The axial force excites the axisymmetric zeroth circumferential modes of the hull, but the radial component excites all circumferential order modes. The steady state response of the structure is calculated by assembling the matrix of the boundary and continuity conditions. The sound radiation is calculated solving the Helmholtz integral in the far field. For the $n=1$ circumferential bending modes, the sound pressure in the axial direction becomes insignificant since the hull displacement is mainly radial, resulting in large pressure lobes normal to the hull. For validity of the present study, analytical results are compared with computational results obtained from a fully coupled finite element/boundary element model developed using Nastran and Sysnoise.

STRUCTURAL MODEL OF THE SUBMARINE

The submarine hull is modelled as a cylindrical shell with internal bulkheads and ring stiffeners. The cylindrical shell is closed by truncated conical shells, which in turn are closed at each end by circular plates, as shown in Fig. 1. The entire structure is submerged in a heavy fluid medium.

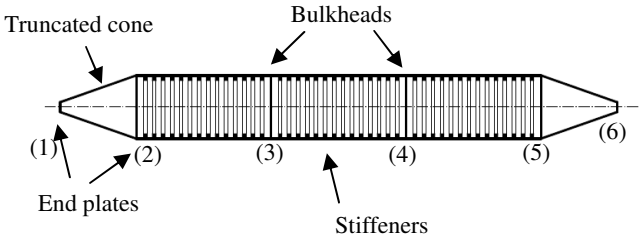

Figure 1. Schematic diagram of the submarine

Using Flügge thin shell theory, the equations of motion and general solutions for the fluid loaded cylindrical and conical shells and for the circular plates were presented previous by the authors (Caresta et al. 2008). The cylindrical shell displacements are given by (Leissa 1993)

$$u = \sum_{n=0}^{\infty}\sum_{i=1}^{8} C_{n,i} W_{n,i} e^{jk_{n,i}x} \cos(n\theta) e^{-j\omega t} \tag{1}$$

$$v = \sum_{n=0}^{\infty}\sum_{i=1}^{8} G_{n,i} W_{n,i} e^{jk_{n,i}x} \sin(n\theta) e^{-j\omega t} \tag{2}$$

$$w = \sum_{n=0}^{\infty}\sum_{i=1}^{8} W_{n,i} e^{jk_{n,i}x} \cos(n\theta) e^{-j\omega t} \tag{3}$$

where *u*, *v* and *w* are respectively the axial, circumferential and radial components of the cylindrical shell displacements.

The conical shell displacements can be written as (Tong 1993)

$$u_c(x_c,\theta_c,t)=\sum_{n=0}^{\infty}\mathbf{u}_{c,n}\cdot\mathbf{x}_{c,n}\cos(n\theta_c)e^{-j\omega t} \quad (4)$$

$$v_c(x_c,\theta_c,t)=\sum_{n=0}^{\infty}\mathbf{v}_{c,n}\cdot\mathbf{x}_{c,n}\sin(n\theta_c)e^{-j\omega t} \quad (5)$$

$$w_c(x_c,\theta_c,t)=\sum_{n=0}^{\infty}\mathbf{w}_{c,n}\cdot\mathbf{x}_{c,n}\cos(n\theta_c)e^{-j\omega t} \quad (6)$$

u_c, v_c, and w_c are the orthogonal components of the conical shell displacements. $\mathbf{x}_{c,n}$ is the vector of the eight unknown coefficients for a specific circumferential mode number *n*. $\mathbf{u}_{c,n}$ $\mathbf{v}_{c,n}$ and $\mathbf{w}_{c,n}$ are the x_c–dependent components of the conical shell displacements expressed in terms of a power series, where x_c is the direction of the cone along its generator (Caresta and Kessissoglou 2008).

General solutions for the bending and in-plane motions of a thin circular plate are given by (Tso and Hansen 1995)

$$w_p=\sum_{n=0}^{\infty}\left(A_{n,1}J_n(k_{pB}r)+A_{n,2}I_n(k_{pB}r)\right)\cos(n\theta_p)e^{-j\omega t} \quad (7)$$

$$v_p=-\sum_{n=0}^{\infty}\left(\frac{nB_{n,1}J_n(k_{pL}r)}{r}+B_{n,2}\frac{\partial J_n(k_{pT}r)}{\partial r}\right)\sin(n\theta_p)e^{-j\omega t} \quad (8)$$

$$u_p=\sum_{n=0}^{\infty}\left(B_{n,1}\frac{\partial J_n(k_{pL}r)}{\partial r}+\frac{nB_{n,2}J_n(k_{pT}r)}{r}\right)\cos(n\theta_p)e^{-j\omega t} \quad (9)$$

where w_p, u_p and v_p are respectively the axial, radial and circumferential plate displacements. k_{pB} is the plate bending wavenumber and k_{pL}, k_{pT} are the wavenumbers for in-plane waves in the plate (Tso and Hansen 1995). J_n and I_n are respectively Bessel functions and modified Bessel functions of the first kind. The coefficients $A_{n,i}$ and $B_{n,i}$ ($i=1,2$) are determined from the boundary conditions of the circular plates.

The dynamic response of the entire submarine structure for each circumferential mode number *n* is expressed in terms of the radial wave amplitudes $W_{n,i}$ ($i=1:8$) for each section of the hull, the wave amplitudes $A_{n,i}$, $B_{n,i}$ ($i=1,2$) for each circular plate, and eight unknown coefficients $\mathbf{x}_{c,n}$ for each piece of frustum of cone. The dynamic responses for the cylindrical shells, circular plates and conical shells using the two different techniques (wave approach and power series) can be coupled together by continuity of the displacements and slope, and equilibrium of forces and moments at the cone/plate/cylinder junctions. The forces, moments, displacements and slope at the junctions and boundaries of the coupled shells and plates are given in accordance with the sign convention shown in Figure 2, where RC_0 is the global Cartesian reference frame. The membrane forces (N_x, N_θ, $N_{x\theta}$), bending moments (M_x, M_θ, $M_{x\theta}$), transverse shearing Q_x for the shells and plates are given in Leissa (1993).

To take into account the change of curvature between the cylinder and the cone, the following notation was introduced

$$\tilde{u}_c=u_c\cos\alpha-w_c\sin\alpha \quad (10)$$

$$\tilde{w}_c=w_c\cos\alpha+u_c\sin\alpha \quad (11)$$

$$\tilde{N}_{x,c}=N_{x,c}\cos\alpha-V_{x,c}\sin\alpha \quad (12)$$

$$\tilde{V}_{x,c}=V_{x,c}\cos\alpha+N_{x,c}\sin\alpha \quad (13)$$

At the cone/circular plate/cylinder junctions corresponding to junctions (2) in Figure 1, the continuity conditions are given by

$$u=\tilde{u}_c=w_p \quad (14)$$

$$w=\tilde{w}_c=u_p \quad (15)$$

$$v=v_c=v_p \quad (16)$$

$$-\phi=-\phi_c=\phi_p \quad (17)$$

$$-N_x-\tilde{N}_{x,c}+N_{x,p}=0 \quad (18)$$

$$-\left(N_{x\theta}+\frac{M_{x\theta}}{a}\right)+\left(N_{x\theta,c}+\frac{M_{x\theta,c}}{a}\right)+N_{\theta,p}=0 \quad (19)$$

$$-M_x+M_{x,c}-M_{x,p}=0 \quad (20)$$

$$-V_x+\tilde{V}_{x,c}+N_{r,p}=0 \quad (21)$$

The Kelvin-Kirchhoff shear forces $V_x, V_{x,c}$ are given by

$$V_x=Q_x+\frac{1}{a}\frac{\partial M_{x\theta}}{\partial\theta},\ V_{x,c}=Q_{x,c}+\frac{1}{R(x_c)}\frac{\partial M_{x\theta,c}}{\partial\theta_c} \quad (22)$$

At the free ends of the truncated cones corresponding to junctions (1) in Figure 1, similar expressions for the continuity conditions between the conical shells and circular plates can be used.

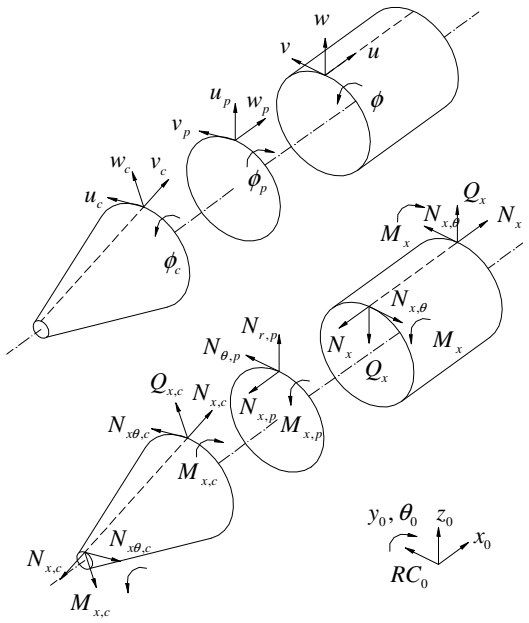

Figure 2. Sign convention for the forces, moments and displacements of the cones, cylinder and circular plates.

The steady state response of the hull can be calculated considering the force as part of the boundary conditions. With a radial harmonic force, the continuity condition of radial forces at the end plate/cone junction (1) becomes

$$-\tilde{V}_{x,c}\Big|_{x_0} + N_{r,p}\Big|_{x_0} = \varepsilon F_0 \cos(n\theta_0) \quad (23)$$

where $F_0 = 1$ and $\varepsilon = 1/2\pi R_1$ if $n = 0$ and $\varepsilon = 1/\pi R_1$ if $n \neq 0$.

.

FAR FIELD SOUND PRESSURE

Acoustic model of the submarine has been presented previously by the authors (Caresta et al. 2008). The sound pressure at a far field location was solved by means of the Helmholtz integral formulation. The far field is located in spherical coordinates, as shown in Figure 3.

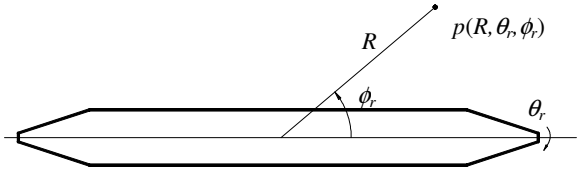

Figure 3. Coordinate system for the far field point.

RESULTS

Results are presented for a ring stiffened cylindrical shell of radius $a = 3.25$ m, thickness $h = 0.04$ m, length $L = 45$ m and with two evenly spaced bulkheads of thickness $h_p = 0.04$ m. A distributed mass on the cylinder $m_{eq} = 1500\ \mathrm{kgm}^{-2}$ has been considered to account for the onboard equipment and ballast tanks (Tso and Jenkins 2003). The internal stiffeners have a rectangular cross-section of $0.08\mathrm{m} \times 0.15\mathrm{m}$ and are evenly spaced by $b = 0.5$ m. The truncated conical shells have a small radius of $R_1 = 0.50$ m, semi-vertex angle of $\alpha = 18°$ and thickness $h_c = 0.014$ m. All the structures are made of steel, with density $\rho = 7800\ \mathrm{kgm}^{-3}$, Young's modulus $E = 2.1\times10^{11}\ \mathrm{Nm}^{-2}$ and Poisson's ratio $\upsilon = 0.3$. A complex Young modulus of $E = E(1 - j\eta)$, where $\eta = 0.02$ is the structural loss factor, is considered to account for the structural damping. The acoustic results are presented in terms of the maximum sound pressure defined by $P_{\max} = \max_{0\le\phi_r\le2\pi}\left(p(R,\theta_r)\right)$ evaluated in the far field at $\theta_r = 0$ and R = 1000 m.

Propeller shaft excitation

Results for the structural responses of the submarine hull under excitation from the propeller-shafting system are presented. The fluctuating forces at the propeller due to rotation of the propeller through a non-uniform wake are transmitted through the propulsion system, resulting in excitation of the cylindrical hull at its end plate. The fluctuating forces in the axial and radial directions are of similar magnitude (Breslin and Andersen 1994). In this analysis, the dynamics of the propeller-shafting system has not been considered and its influence is simplified as follows. The axial force is considered to be transmitted directly to the hull exciting the axisymmetric modes of the submarine. The radial component is approximated as a point force applied to the extremity of the end cone. The total excitation acting on the hull is contributed by an axisymmetric distributed load $D_x = F_a / 2\pi a$ [Nm^{-1}] where F_a is an axial force applied at the end plate of the cylindrical shell (junction 2 in Figure. 1), and a point radial force F_r applied at the end plate of the conical shell (junction 1 of Figure. 1), as shown in Figure 4.

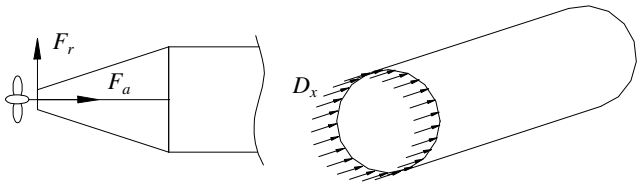

Figure 4. Fluctuating forces from the propeller.

Structural responses

Figure 5 presents the frequency response function (FRF) of the axial displacement at the cone/cylinder junction corresponding to the location of the distributed force. In the case of an axisymmetric excitation (D_x), only the $n = 0$ accordion modes are excited. It can be seen the first three resonant frequencies occur at frequencies of around 22.5, 44.5 and 68.5 Hz. The small peaks at around 9 Hz and 37 Hz are due to the resonances of the bulkheads. Under radial point force excitation (F_r), the response is dominated by the $n = 1$ bending modes.

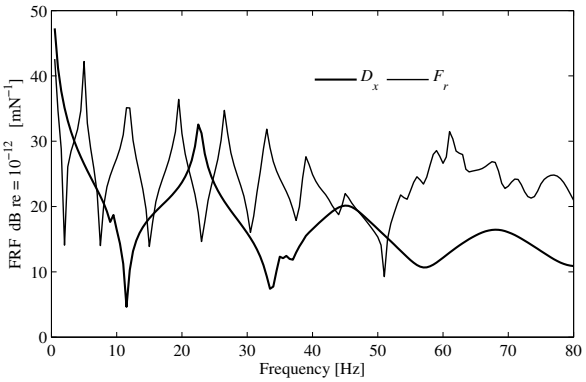

Figure 5. Axial displacement at the end plate of the cylindrical shell, $n = 0:30$.

Modeshapes at the third, fourth and fifth *n*=1 resonances excited by the radial force are shown in Figures 6 to 8. The corresponding frequencies are 19.5, 26.5 and 33 Hz, respectively. Due to the flexural motion of the cones, the ends of the hull are shown to be vibrating in phase or out or phase with each other. Under point radial force excitation, an increase in the structural response is observed in Figure 5 at around 61 Hz. This is due to the cutting-on of the second class of waves (Class II). Figure 9 presents the structural wavenumbers k_n of the cylindrical shell of the hull for *n*=1 modes. The mainly real wavenumbers represent travelling waves in the structure; their small imaginary part is due to both structural damping and fluid-loading. While the first class of waves (CL I) cuts-on at 0 Hz, it can be observed that the cutting-on of the second class of waves (CL II) occurs at around 61 Hz. The CL II waves fall in the supersonic region of the wavenumber spectrum ($k_n < k_f$), thus a stronger contribution to the sound radiation occurs. At 61 Hz, the operational deformation shape is mainly determined by *n*=1 bending modes of the hull and a very strong deformation for the end cones is observed, as shown in Figure 10.

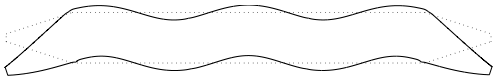

Figure 6. Operational deformation shape at the third $n=1$ bending resonant frequency of 19.5 Hz.

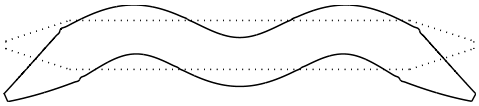

Figure 7. Operational deformation shape at the fourth $n=1$ bending resonant frequency of 26.5 Hz.

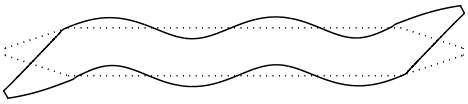

Figure 8. Operational deformation shape at the fifth $n=1$ bending resonant frequency of 33.0 Hz.

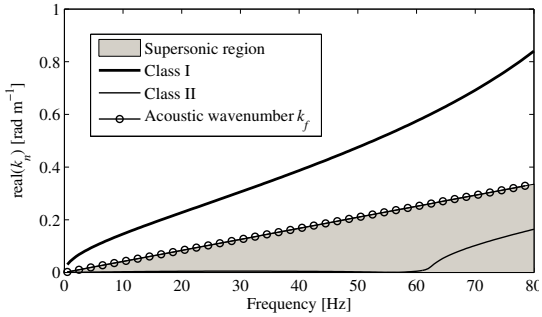

Figure 9. Real part of the structural wavenumbers for the n=1 bending modes.

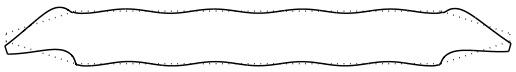

Figure 10. Operational deformation shape at 61 Hz.

For validity of the present study, the structural and acoustic responses of the submarine were compared with results from a fully coupled computational model. A finite element (FE) model was solved using Nastran for a structure *in vacuo* and a boundary element (BE) model was developed using Sysnoise for a fluid-loaded structure. Figures 11 and 12 present the frequency response functions (FRFs) of the axial displacement at the end plate of the cylindrical shell under radial excitation (Fig. 11), and under an axisymmetric distributed load (Fig. 12). Figure 11 presents the FRFs for both the *in vacuo* and fluid loaded cases. No difference between the analytical and computational results is observed for the *in vacuo* case while some small discrepancies occur with fluid-loading. These discrepancies are attributed to low frequency approximations for the fluid loading in the analytical model. It can be observed that fluid loading reduces both the value of the natural frequencies and the amplitude of the FRF. Figure 12 shows that for the axisymmetric case, only small differences between the analytical and computational results can be observed. The smooth peaks at the second and third hull resonances are due to the damping effect of the fluid loading.

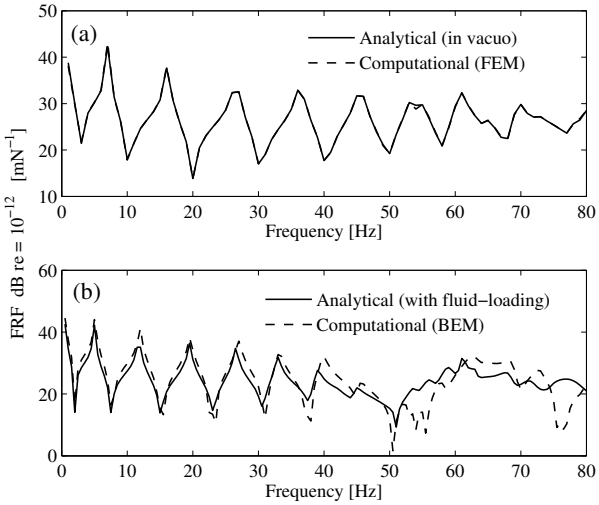

Figure 11. Axial displacement at the end plate of the cylindrical shell under radial excitation, (a) *in vacuo* case, (b) with fluid-loading.

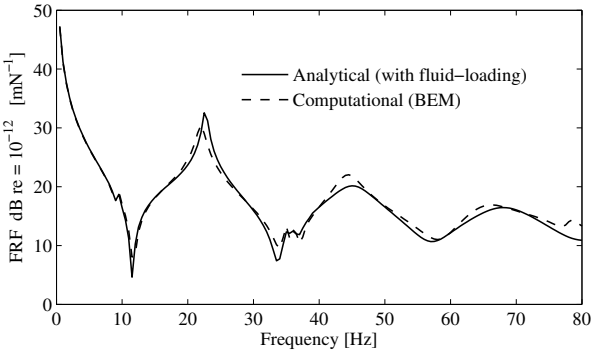

Figure 12. Axial displacement at the end plate of the cylindrical hull under an axisymmetric.

Acoustic responses

Figure 13 presents the maximum sound pressure in the far field defined by $P_{\max} = \max_{0\le\phi_r\le 2\pi}\left(p(R,\theta_r)\right)$ due to an axisymmetric distributed load (D_x) and under point radial excitation (F_r). It can be seen that the radial force at the end plate of the conical shell significantly contributes to the sound radiation, especially above 30 Hz. Modes with $n \ge 2$ do not contribute significantly to the sound radiated to the far field. At around 61 Hz when the cutting-on of the CLII waves occurs, an increase in sound radiation is observed.

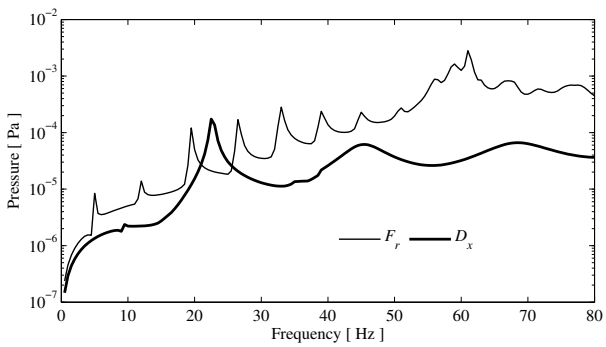

Figure 13. Maximum far field sound pressure, R = 1000m, $\theta_r = 0$.

Radiation directivity patterns

For the axisymmetric case, the radiation directivity patterns corresponding to the first three axial resonant frequencies are shown in Figures 14 to 16 for $\theta_r = 0$ and $0 \le \phi_r \le 180^\circ$. Also shown are the individual contributions to the radiated sound pressure from the cylindrical and conical shells. The contribution from the cylindrical shell is represented by the central lobes in the directivity patterns, whereas the large side lobes are due to the contribution from the end cones. As the frequency increases, the radiation directivity patterns increase in complexity. For the first three axial resonances, there are one, two and three central lobes, respectively. Due to the phase relationship between the pressure fields generated by the cylindrical and conical shells, the total sound pressure is the greatest along the axial direction for the first two axial resonant frequencies. A partial cancellation occurs in the direction normal to the axis of the submarine.

The directivity patterns obtained computationally using Sysnoise are also shown in Figure 14 for the first axial resonant frequency and in Figure 17 for the second and third axial resonant frequencies. Very good agreement between the analytical and computational results is observed at the first and third resonant frequencies. The difference in magnitude between the analytical and computational results is attributed to the differences in the magnitude of the structural responses as observed in Fig. 12, but the general directivity shape is preserved.

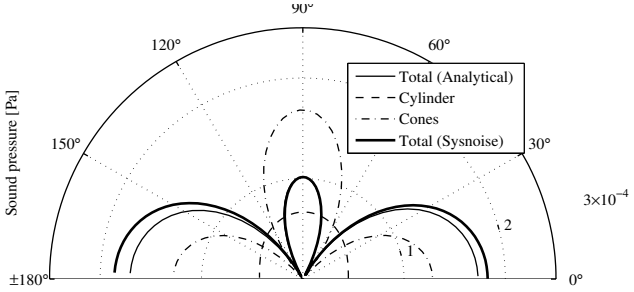

Figure 14. Radiated sound pressure at the first $n = 0$ axial resonant frequency of 22.5 Hz (analytical and computational results).

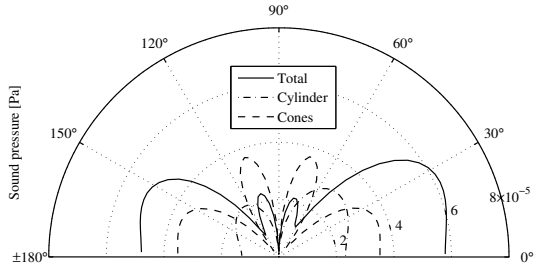

Figure 15. Radiated sound pressure at the second $n = 0$ axial resonant frequency of 45.5 Hz (analytical result).

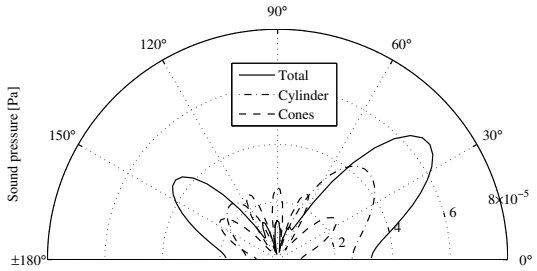

Figure 16. Radiated sound pressure at the third $n = 0$ axial resonant frequency of 68.5 Hz (analytical result).

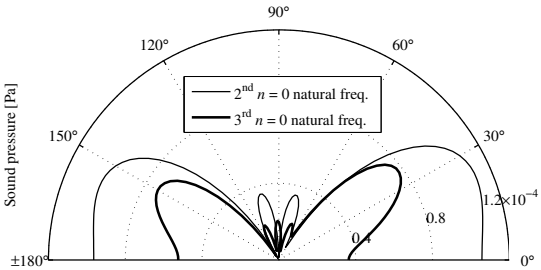

Figure 17. Radiated sound pressure at the second and third axial resonant frequencies (computational results).

Radiation directivity patterns for the third, fourth and fifth $n = 1$ modes of the hull, corresponding to frequencies of 19.5, 26.5 and 33 Hz respectively, are shown in Figures 18 to 20. The general directivity shapes obtained analytically and computationally are very similar, showing reduced radiated sound pressure along the axis of the hull and large lobes normal to the hull. The difference in magnitude between the analytical and computational results is attributed to the differences in the magnitude of the structural responses, as observed in Figure 11(b). For the frequency range of interest, the maximum radiated sound pressure was shown to occur at around 61 Hz, due to the cutting-on of the CLII waves. The directivity pattern of the radiated sound pressure at 61 Hz is presented in Fig. 21. The sound pressure is less significant in the axial direction since the hull displacement is mainly radial.

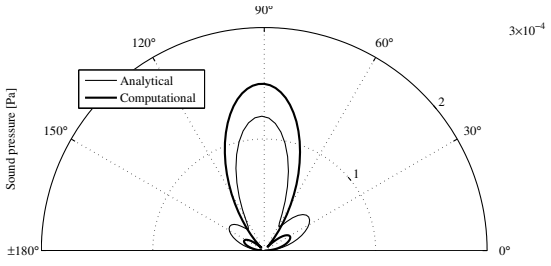

Figure 18. Radiated sound pressure at the third $n = 1$ bending resonant frequency of 19.5 Hz (analytical and computational results).

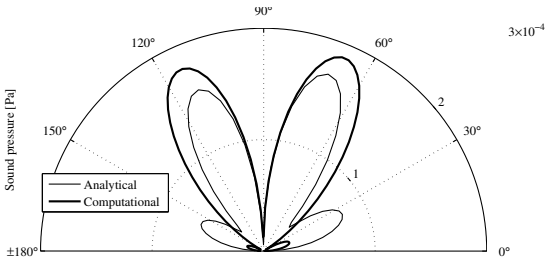

Figure 19. Radiated sound pressure at the fourth $n=1$ bending resonant frequency of 26.5 Hz (analytical and computational results).

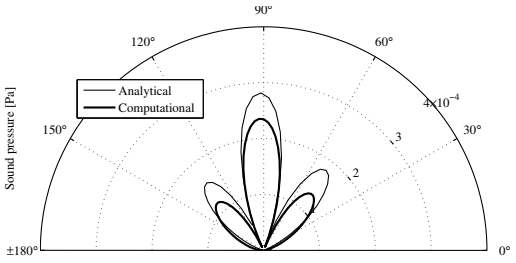

Figure 20. Radiated sound pressure at the fifth $n=1$ bending resonant frequency of 33 Hz (analytical and computational results).

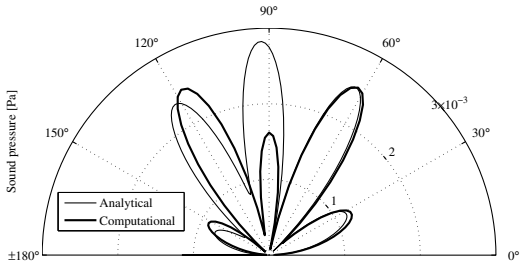

Figure 21. Radiated sound pressure at 61 Hz (analytical and computational results).

CONCLUSIONS

The vibro-acoustic responses of a submerged vessel in the low frequency range have been presented using a semi-analytical model. The structural response of the submarine under point force excitation was obtained by assembling the boundary/continuity matrix. The surface displacement and pressure were used in the Helmholtz integral formulation to evaluate the far-field radiated sound pressure. Excitation from the propeller was modelled as a fluctuating radial point force on the stern side of the submarine and a distributed axisymmetric load acting on the cylindrical hull. It was shown that excitation due to the radial force results in greater sound pressure radiated to the far-field compared with the sound radiation due to axisymmetric excitation of the hull. This is due to the $n=1$ circumferential bending modes. Furthermore, in the frequency range of interest, the greatest sound radiation was found to occur at the frequency corresponding to the cutting-on of the second class of waves for the $n=1$ modes. This is associated with supersonic waves in the structure and an increase in the global structural response. The importance of the $n=1$ bending modes in the sound pressure radiated by a submarine under harmonic excitation from the propulsion system was shown.

REFERENCES

Achenbach, J.D., Bjarnason, J. and Igusa, T. (1992) *Effect of a vibrating substructure on acoustic radiation from a cylindrical shell*. Journal of Vibration and Acoustics, Transactions of the ASME, 114, 312-318.

Alfredson, R.J. (1973) *A note on the use of the finite difference method for predicting steady state sound fields*. Acoustica, 28, 296-301.

Arlette, P.L., Bahrani, A.K. and Zienkiewicz, O.C. (1968) *Application of FEM to solution of Helmholtz's equation*. Proc. IEEE, 115, 1766-1768.

Bjarnason, J., Igusa, T., Choi, S.-H. and Achenbach, J.D. (1994) *The effect of substructures on the acoustic radiation from axisymmetric shells of finite length*. Journal of the Acoustical Society of America, 96, 246-255.

Breslin, J.P. and Andersen, P. (1994) *Hydrodynamics of ship propellers*, Cambridge University Press.

Caresta, M., Kessissoglou, N.J. and Tso, Y.K. (2008) *Low frequency structural and acoustic responses of a submarine hull*, Acoustics Australia, 36, 47-52.

Caresta, M. and Kessissoglou, N.J. (2008) *Vibration of fluid loaded conical shells*. Journal of the Acoustical Society of America, 124, 2068-2077.

Chen, H.-W. and Stepanishen, P. (1994) *Acoustic transient radiation from fluid-loaded shells of revolution using time-dependent in vacuo eigenvector expansions*. Journal of the Acoustical Society of America, 95, 601-16.

Chen, P.-T. and Ginsberg, J.H. (1993) *Variational formulation of acoustic radiation from submerged spheroidal shells*. Journal of the Acoustical Society of America, 94, 221-33.

Chertock, G. (1975) *Sound radiated by low-frequency vibrations of slender bodies*. Journal of the Acoustical Society of America, 57, 1007-1016.

Chien, C.C., Rajiyah, H. and Atluri, S.N. (1990) *An effective method for solving the hypersingular integral equations in 3-D acoustics*. Journal of the Acoustical Society of America, 88, 918-37.

Choi, S.H., Igusa, T. and Achenbach, J.D. (1995) *Nonaxisymmetric vibration and acoustic radiation of a submerged cylindrical shell of finite length containing internal substructures*. Journal of the Acoustical Society of America, 98, 353-362.

Choi, S.H., Igusa, T. and Achenbach, J.D. (1996) *Acoustic radiation from a finite-length shell with non-axisymmetric substructures using a surface variational principle*. Journal of Sound and Vibration, 197, 329-350.

Hue-Wang, C. and Stepanishen, P. (1994) *Acoustic transient radiation from fluid-loaded shells of revolution using time-dependent in vacuo eigenvector expansions*. Journal of the Acoustical Society of America, 95, 601-16.

Jeans, R.A. and Mathews, I.C. (1990) *Solution of fluid-structure interaction problems using a coupled finite element and variational boundary element technique*. Journal of the Acoustical Society of America, 88, 2459-66.

Jeans, R.A. and Mathews, I.C. (1993) *A unique coupled boundary element/finite element method for the elastoacoustic analysis of fluid-filled thin shells*. Journal of the Acoustical Society of America, 94, 3473-9.

Junger, M.C. and Feit, D. (1986) *Sound, structures, and their interaction*, Cambridge, Mass., MIT Press.

Leissa, A.W. (1993) *Vibration of shells*, New York, American Institute of Physics.

Pan, X., Tso, Y. and Juniper, R. (2008a) *Active control of low-frequency hull-radiated noise*. Journal of Sound and Vibration, 313, 29-45.

Pan, X., Tso, Y. and Juniper, R. (2008b) *Active control of radiated pressure of a submarine hull*. Journal of Sound and Vibration, 311, 224-242.

Pei-Tai, C. and Ginsberg, J.H. (1993) *Variational formulation of acoustic radiation from submerged spheroidal shells*. Journal of the Acoustical Society of America, 94, 221-33.

Pond, H.L. (1966) *Low-frequency sound radiation from slender bodies of revolution*. Journal of the Acoustical Society of America, 40, 711-720.

Stepanishen, P.R. (1997) *Acoustic axisymmetric radiation and scattering from bodies of revolution using the internal source density and Fourier methods*. Journal of the Acoustical Society of America, 102, 726-732.

Tong, L. (1993) *Free vibration of orthotropic conical shells*. International Journal of Engineering Science, 31, 719-33.

Tso Y.K. and Hansen, C.H. (1995) *Wave propagation through cylinder/plate junctions*. Journal of Sound and Vibration, 186, 447-461.

Tso, Y.K. and Jenkins, C.J. (2003) *Low frequency hull radiation noise*. Report No. Dstl/TR05660, Defence Science and Technology Organisation, UK.

Wu, X.-F. (1989) *Faster calculations of sound radiation from vibrating cylinders using variational formulations*. Journal of Vibration, Acoustics, Stress, and Reliability in Design, 111, 101-106.